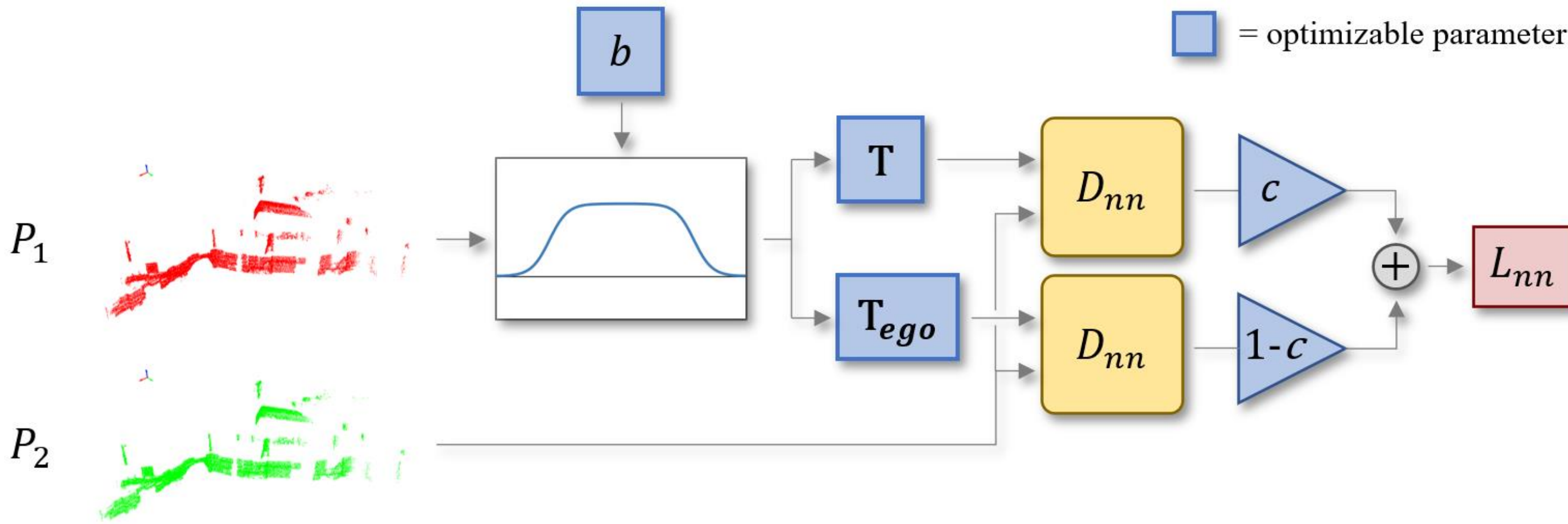




RSF: Optimizing Rigid Scene Flow From 3D Point Clouds Without Labels

David Deng and Avidesh Zakhor
University of California, Berkeley



Scene Flow Parameters

$$\mathbf{T}_{ego} \in SE(3), \mathbf{T}_i \in SE(3)$$

$$\mathbf{b}_i = \{c_i, x_i, y_i, z_i, w_i, l_i, h_i, \theta_i\}$$

for $i = 1 \dots k$

c_i = confidence, $\{x_i, y_i, z_i\}$ = position,
 $\{w_i, l_i, h_i\}$ = dimensions, θ_i = heading angle,
 k = number of boxes

Overview of our loss function for a single bounding box. Terms in blue blocks are optimizable scene flow parameters. b : bounding box parameters, \mathbf{T} : bounding box's rigid transformation, \mathbf{T}_{ego} : ego-motion transformation, c : box's confidence score, and the plot refers to our differentiable bounding box approximation. From P_1 , we differentiably select the points inside the bounding box and transform them using \mathbf{T} and \mathbf{T}_{ego} . Then we compute the nearest neighbor distance (NND) between the two transformed point sets and P_2 . Lastly, we weigh the two NNDs by c and $1-c$ respectively and sum them to compute the loss. Our total loss is the sum of per box losses in addition to shape, heading, angle, and mass auxiliary losses.

Problem

Given a pair of 3D point clouds, predict the scene flow between them without any labels.

Image taken from [1].

Background

- Self-supervised scene flow from point clouds
 - Minimize NND over pointwise motion vectors
 - Smoothness and geometry regularization, cycle consistency
- Optimization based approaches
 - Neural Scene Flow Prior [2] trains a DNN for each scene, using it as an implicit regularizer

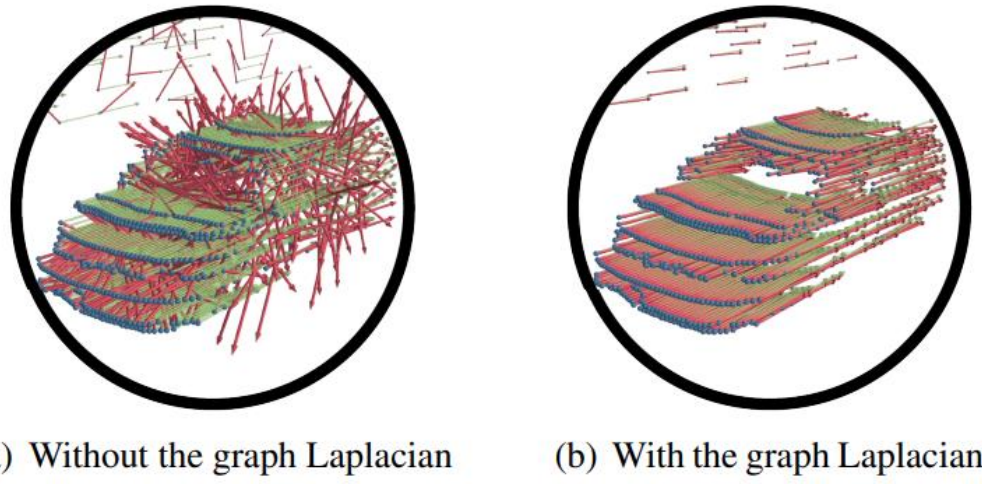


Image taken from [3]

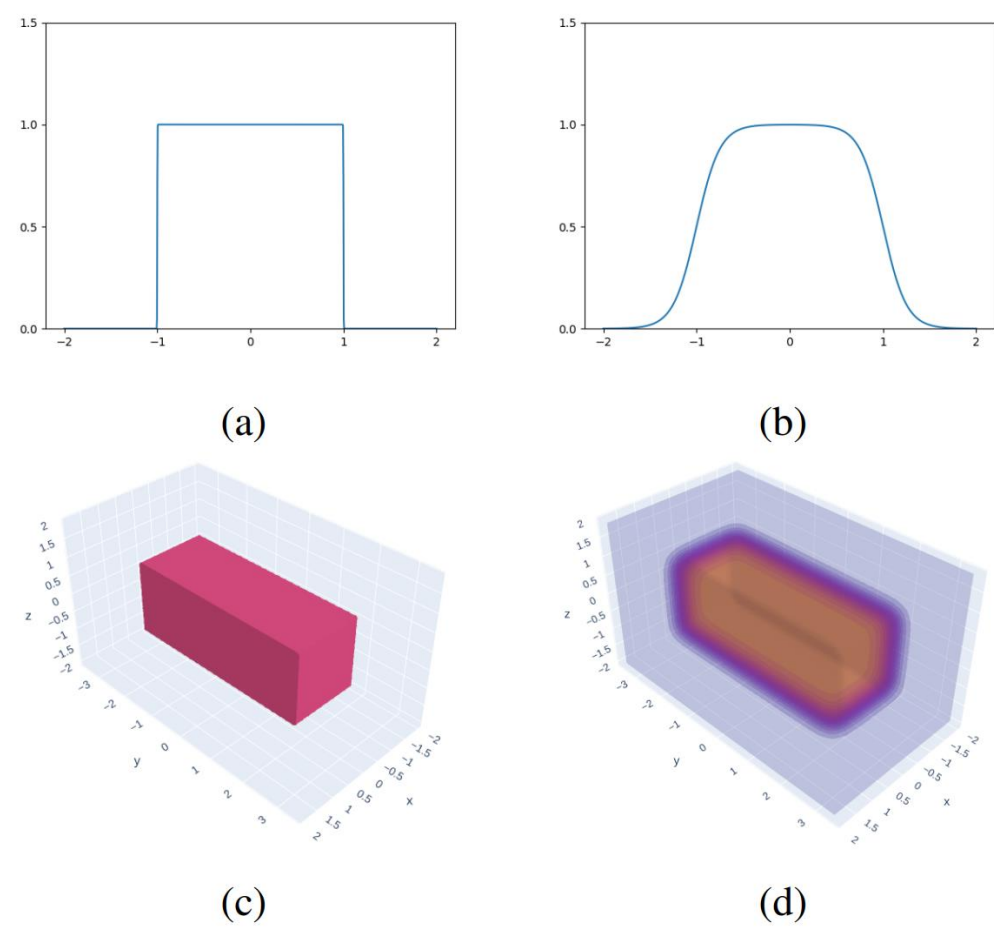
Approach

Observation: scenes are comprised of independently moving rigid objects

Instead of pointwise vectors, we parameterize scene flow at the object level and parameterize objects as bounding boxes

- Lower dimension optimization space
- Constrains scene flow to be physically coherent
- Solve for parameters by optimizing them over the NND with gradient methods

Differentiable Bounding Boxes

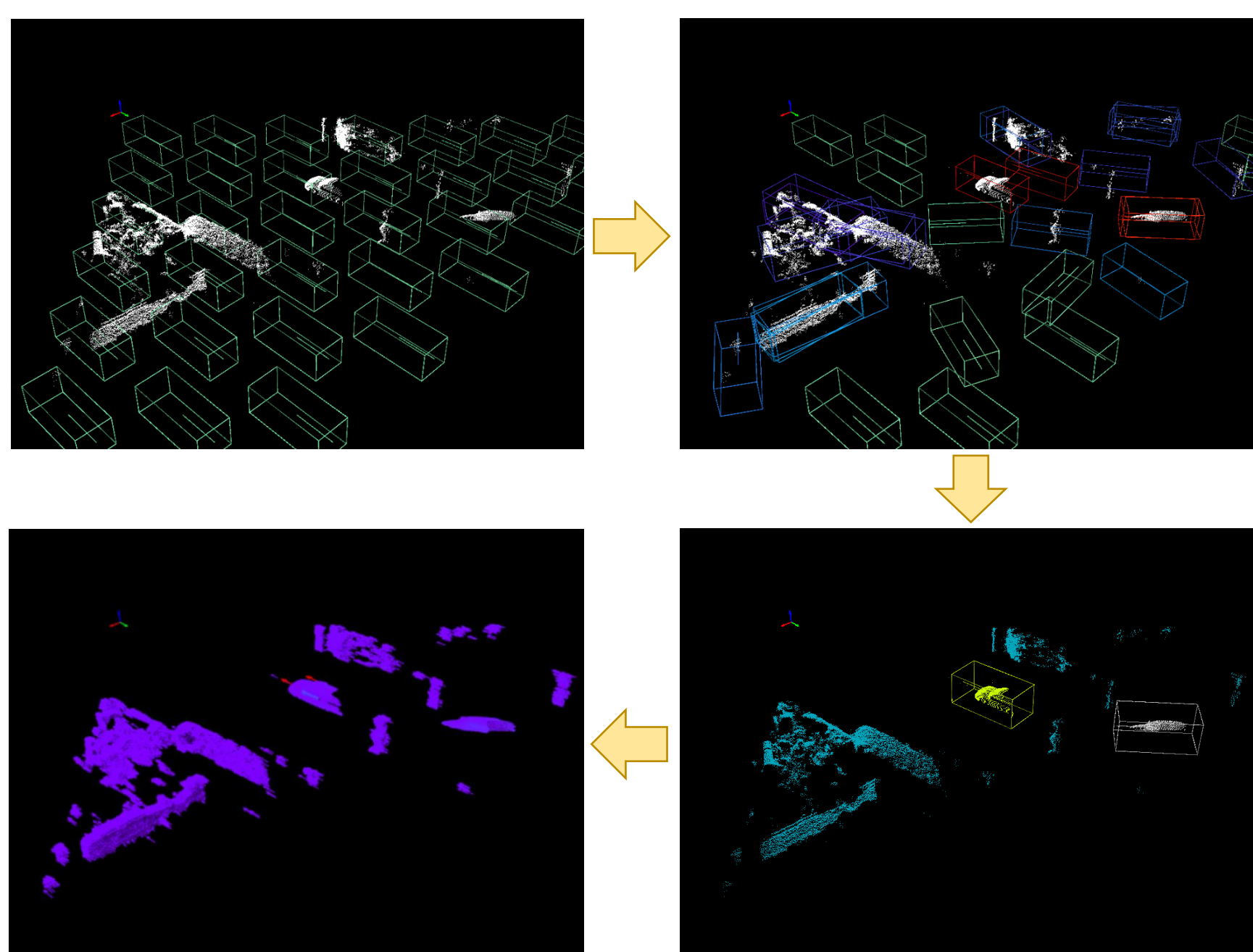


Visualizations of non-differentiable vs differentiable bounding boxes in 1 and 3 dimensions: (a) non-differentiable 1D bounding line; (b) differentiable 1D bounding line; (c) non-differentiable 3D bounding box; (d) differentiable 3D bounding box.

Inference

Post processing: prune empty boxes, non-maximum suppression, assign points to objects

Scene flow: $\mathbf{f}_i = \mathbf{R}_i \mathbf{p}_i + \mathbf{t}_i - \mathbf{p}_i$



Results

Table 1: Scene flow evaluation.

Dataset	Method	Supervision/ Approach	Training Data	EPE3D ↓	Acc3DS ↑	Acc3DR ↑	Outliers ↓
StereoKITTI	FlowNet3D [27]	Full	FT3D	0.177	0.374	0.668	0.527
	HPLFlowNet [13]	Full	FT3D	0.117	0.478	0.778	0.410
	PointPWCNet [50]	Full	FT3D	0.069	0.728	0.888	0.265
	FLOT [36]	Full	FT3D	0.056	0.755	0.908	0.242
	EgoFlow [54]	Full	FT3D	0.069	0.670	0.879	0.404
	FlowStep3D [51]	Full	FT3D	0.055	0.805	0.925	0.149
	HCRF-Flow [39]	Full	FT3D	0.053	0.863	0.944	0.180
	WeaklyRigidFlow [12]	Full	FT3D	0.042	0.849	0.959	0.208
	PointPWCNet [50]	Self	FT3D	0.255	0.238	0.496	0.686
	EgoFlow [54]	Self	FT3D	0.415	0.221	0.372	0.810
	FlowStep3D [51]	Self	FT3D	0.102	0.708	0.839	0.246
	SLIM [1]	Self	RawKITTI	0.121	0.518	0.796	0.402
	SLIM*[1]	Self	RawKITTI	0.067	0.77	0.934	0.249
	RigidFlow [24]	Self	FT3D	0.062	0.724	0.892	0.262
	Chamfer*	Optimization	-	0.991	0.056	0.071	0.942
	PointPWCNet [50]	Optimization	-	0.657	0.357	0.405	0.72
	NSFP [25]	Optimization	-	0.036	0.912	0.961	0.154
	NSFP*[25]	Optimization	-	0.034	0.914	0.962	0.151
	Ours	Optimization	-	0.035	0.932	0.971	0.146
	Ours*	Optimization	-	0.017	0.973	0.989	0.096
LidarKITTI	PointPWCNet [50]	Full	FT3D	0.390	0.387	0.550	0.653
	FLOT [36]	Full	FT3D	0.653	0.155	0.313	0.837
	WeaklyRigidFlow [12]	Weak	SemKITTI	0.094	0.784	0.885	0.314
	ExploitingRigidity [8]	Weak	SemKITTI	0.071	0.824	0.913	0.295
	Chamfer*	Optimization	-	0.944	0.022	0.057	0.992
	PointPWCNet [50]	Optimization	-	0.734	0.248	0.347	0.845
nuScenes	NSFP*[25]	Optimization	-	0.142	0.688	0.826	0.385
	Ours*	Optimization	-	0.085	0.883	0.929	0.239
	Chamfer*	Optimization	-	0.879	0.035	0.082	0.976
	PointPWCNet*[50]	Optimization	-	0.615	0.199	0.328	0.86
	NSFP [25]	Optimization	-	0.177	0.374	0.668	0.527
	Ours*	Optimization	-	0.107	0.717	0.862	0.321

* methods that use the entire point cloud. All other methods downsample to 8,192 points.

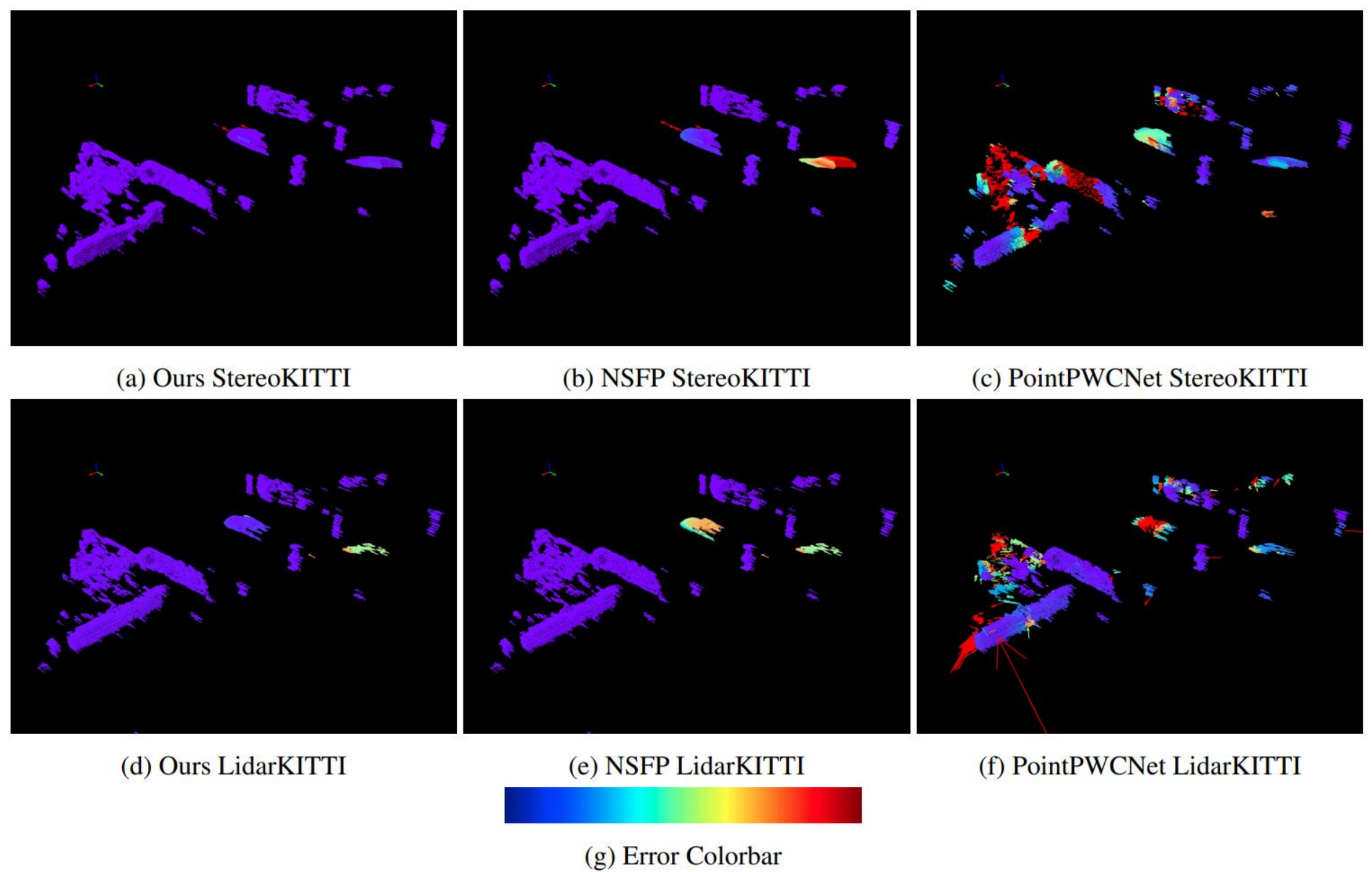
Table 2: Motion segmentation results on StereoKITTI.

Method	mIoU ↑	Accuracy ↑
SLIM [1]	42.9	60.1
Ours	86.6	92.9

Table 3: Ego-Motion Estimation Evaluation on SemanticKITTI.

Method	Rotation Error (°) ↓	Translation Error (m) ↓	Rotation Accuracy ↑	Translation Accuracy ↑
ICP [3]	0.244	0.122	0.906	0.878
Ours	0.235	0.107	0.916	0.94

Visualizations



Visualization of scene flow predictions for our method, NSFP, and the PointPWCNet loss function under direct optimization on a scene in KITTI. Color indicates the EPE3D of the prediction, with red indicating high error and purple indicating low error. For StereoKITTI, the colorscale ranges from 0-0.5 m error, while for LidarKITTI, it ranges from 0-1 m.

Conclusion

We propose a novel method for optimizing object-level rigid scene flow without labels. Our method achieves state-of-the-art accuracy by constraining the scene flow to be physically consistent, and it simultaneously detects moving objects and computes ego-motion without any labels.

References

- [1] Xingyu Liu, Charles R Qi, and Leonidas J Guibas. FlowNet3d: Learning scene flow in 3d point clouds. In *In Computer Vision and Pattern Recognition (CVPR)*, 2019.
- [2] Xueqian Li, Jhony Kaesemodel Pontes, and Simon Lucey. Neural scene flow prior. *Advances in Neural Information Processing Systems*, 34, 2021.
- [3] Jhony Kaesemodel Pontes, James Hays, and Simon Lucey. Scene flow from point clouds with or without learning. *International Conference on 3D Vision (3DV)*, 2020.